

**This document is the unedited Author's version of a Submitted Work that was subsequently accepted for publication in The Journal of Physical Chemistry, copyright © American Chemical Society.**

To access the final edited and published work is available online at <https://doi.org/10.1021/jp907443x>

GLOBULIN 11S AND ITS MIXTURE WITH L-DPPC AT THE AIR/LIQUID INTERFACE

Journal:	<i>The Journal of Physical Chemistry</i>
Manuscript ID:	jp-2008-08879e
Manuscript Type:	Article
Date Submitted by the Author:	07-Oct-2008
Complete List of Authors:	Ruiz-Garcia, Jaime; UASLP, Instituto de Fisica Garcia-Gonzalez, Alcione; UASLP, Instituto de Fisica Flores-Vazquez, Ana; UASLP, Instituto de Fisica Maldonado, Enrique; IPICYT, Biologia Molecular Barba De La Rosa, Ana Paulina; Instituto Potosino De Investigation, Biologia Molecular



## 1 2 3 GLOBULIN 11S AND ITS MIXTURE WITH L-DPPC AT THE AIR/LIQUID 4 INTERFACE 5

6  
7 **A. Garcia-Gonzalez**<sup>1,2</sup>, **A. L. Flores-Vazquez**<sup>1</sup>, **E. Maldonado**<sup>3</sup>, **A. P. Barba de la Rosa**<sup>3</sup> and **J. Ruiz-Garcia**<sup>1,\*</sup>  
8

9  
10 <sup>1</sup>*Instituto de Física, Universidad Autónoma de San Luis Potosí, Álvaro Obregón 64, 78000 San Luis Potosí, S.L.P., México.*

11 <sup>2</sup>*Centro de Investigación y Estudios Avanzados del Instituto Politécnico Nacional Unidad Mérida, Antigua carretera Mérida-Progreso km 6, 97310 Mérida, Yucatán*

12 <sup>3</sup>*Instituto Potosino de Investigación Científica y Tecnológica, A.C., Camino a la Presa San José s/n, Lomas 4ª Sección, 78231 San Luis Potosí, S.L.P., México.*  
13  
14  
15  
16

### 17 18 Abstract 19

20 Langmuir films of globulin 11S protein, L-DPPC, and mixtures of both on water and on  
21 buffer subphases were studied. Brewster Angle Microscopy was used to characterize *in*  
22 *situ* the films morphology along  $\pi$ -A isotherms at the air/fluid interface. The L-DPPC  
23 monolayer on water behaved as has been reported extensively in the literature but a slight  
24 increase on surface pressure and a notable change in domain morphology is observed on  
25 buffer. This difference in domain behavior is due to the stabilization interaction of the LE  
26 phase by the buffer ions. On the other hand, the protein monolayer was prepared by direct  
27 deposit or injection below the surface. Both methods formed mostly a condensed film, with  
28 a multilayer formed by globular aggregates in the first method with the two subphases.  
29 However, the second method showed different behavior of the protein films depending on  
30 the subphase; on water the protein formed a homogeneous film with some globule  
31 aggregates, but on buffer a remarkably well organized monolayer was observed by AFM.  
32 Mixtures of globulin 11S and L-DPPC were prepared using both methods for the protein  
33 film formation at the air/fluid interface. BAM showed that the mixtures formed coexistence  
34 regions between two condensed phases, whose domains of both phases behave like  
35 liquids. Fingering phenomena was observed at the interface between protein-rich and L-  
36 DPPC-rich domains, which indicates that both phases are fluid. AFM images of the  
37 mixtures show indeed the formation of protein- or L-DPPC-rich domains. The liquid-like  
38 behavior could be explained due to different sizes of the protein and the L-DPPC, the  
39 minority compound in each kind of domain produces defects making them behave as  
40 liquids. Interestingly enough, as the monolayer is compressed to higher surface pressure,  
41 the lipid molecules are squeezed out and complete separation of the protein and L-DPPC  
42 is produced. Furthermore, we present evidence that the protein/L-DPPC mixtures produce  
43 films with holes, which might indicate its tendency to form hollow aggregates that could  
44 have some relevance in water-channel formation for *in vivo* seed germination.  
45  
46  
47  
48  
49

50  
51 \*Author to whom correspondence should be addressed. e-mail: jaime@ifisica.uaslp.mx  
52  
53  
54  
55  
56  
57  
58  
59  
60

## INTRODUCTION

Langmuir monolayers have been widely used as biological model membranes<sup>1</sup>. In particular, phospholipid monolayers are of great interest as model membranes, mainly due that phospholipids, as well as proteins, are the main structural elements of cell membranes. Surface and interfacial phenomena involving proteins are quite common and of great importance in nature and technology. Therefore, a detailed study of these phenomena is of great interest in biology, chemical technology, biotechnology, and offers new paths in the understanding of protein and polymer chemistry, environmental science. For example, there have been a wide range of studies about protein interface adsorption in a lipidic Langmuir monolayer, although these studies have used mainly food proteins, such as soy<sup>2</sup>, sunflower<sup>3</sup>, Ovoalbumin<sup>4</sup>,  $\beta$ -lactoglobulin<sup>5,6,7</sup>, etc. Indeed, it is possible to study the protein penetration in a lipidic monolayer as a function of superficial pressure; these provide some information about the interactions and structure of protein-lipid layer.

Cornell and Patterson<sup>8</sup> observed the penetration of  $\beta$ -lactoglobulin into mixed Langmuir monolayer of POPC and POPG, at a higher surface pressure than that shown by the pure protein solution, but only a small amount of protein was detected in the mixed films. They observed a binding of  $\beta$ -lactoglobulin at pH 4.4, which is when the protein carries net positive charge but not at higher pH. A similar observation was made by Bos and Nylander<sup>9</sup> for the interaction between  $\beta$ -lactoglobulin and DSPC and DSPA monolayers.

Protein adsorption at a clean air/water interface can also be studied directly as a function of surface pressure as a Langmuir film, which also provides information over the protein structure, interactions and conformation at a hydrophilic/hydrophobic interface. Some

1  
2  
3 examples of pure protein studies involve proteins such as bovine serum albumin<sup>10</sup>,  
4  
5 cytochrome c<sup>11</sup>, apolipoproteins<sup>12</sup>, etc.

6  
7  
8 Moreover, adsorption studies of proteins at fluid-fluid interfaces are essentially motivated  
9  
10 by trying to elucidate structure functionality relationships in emulsifying and foaming food  
11  
12 protein systems<sup>13</sup>. Hence, investigations of protein interfacial layers are of importance for  
13  
14 understanding stability of emulsions and microemulsions when natural high molecular mass  
15  
16 surface-active substances are applied as stabilizers. Colloid chemistry researchers have yet  
17  
18 to get a better understanding on how proteins act as good stabilizers. For example, spatial  
19  
20 structure of protein molecules governs their essential properties, including surface and  
21  
22 biological activity, but in an emulsion or a microemulsion is not always clear if proteins are  
23  
24 folded or unfolded.  
25  
26  
27

28  
29 Storage proteins in seeds are of prominent importance for supplying the world's protein  
30  
31 requirements<sup>14</sup>. It has been shown that seed storage proteins are composed mainly by four  
32  
33 fractions with different physicochemical properties. The major legume storage protein  
34  
35 fractions are globulins, oligomeric globular proteins. The 11S globulins are composed of  
36  
37 six non-covalently linked subunits, each of which contains a disulphide bridge pair of rather  
38  
39 hydrophilic acidic 30-40 kDa  $\alpha$ -polypeptide chain and another hydrophilic basis 20 kDa  $\beta$ -  
40  
41 polypeptide chain. Thus, the molecular weight of the dimeric subunits is 50-60 kDa and  
42  
43 therefore the hexameric protein 300-360 kDa. The oligomeric structure is stabilized by  
44  
45 neutral salts in high ionic strength solution<sup>15</sup>.  
46  
47  
48

49  
50 Amaranth (*Amarantus hypochondriacus*) is a cereal-like crop with high seed yield. The  
51  
52 amaranth seeds has high proteins content (17.9 %)<sup>15</sup> with a better balance of essential  
53  
54 amino acids than those found in cereals and legumes. Therefore, amaranth proteins are one  
55  
56 of the more promising food ingredients, capable of complementing cereal or legume  
57  
58  
59  
60

1  
2  
3 proteins. Amaranth seeds have high proportion of globulins, 22 - 42 % and glutelins 14-18  
4  
5 %<sup>16</sup>, the structure and functionality of these proteins present a strong dependency with the  
6  
7 ionic strength, pH and temperature.  
8  
9

10 On the other hand, the most common way for studying Langmuir monolayers has been  
11  
12 through the measurement of pressure–area isotherms,  $\Pi(A,T) = \gamma^0(T) - \gamma(A,T)$ , where  $T$  is  
13  
14 the temperature,  $A$  is the area/molecule,  $\gamma$  and  $\gamma^0$  are the surface tensions of the monolayer  
15  
16 and of pure water, respectively. There are several techniques that can be also applied  
17  
18 concomitant to observe the monolayer organization at the air/aqueous interface, such as  
19  
20 polarized fluorescence microscopy (PFM)<sup>17,18</sup> and Brewster angle microscopy (BAM)<sup>19</sup>.  
21  
22 These optical techniques are quite sensitive for observing very fine details in Langmuir  
23  
24 monolayers, such as phase transitions, phase coexistence and molecular tilting. For  
25  
26 example, these experimental techniques have revealed that singularities in the surface  
27  
28 pressure–area isotherms are due to phase changes<sup>20,21</sup>. Both techniques have been widely  
29  
30 used to observe the formation of domain structures on monolayers penetrated by  
31  
32 proteins<sup>2,4,7,22,23</sup>. Their lateral resolution is, however, limited by the resolution of the optical  
33  
34 microscope. The transfer of film from the air/aqueous interface to a solid support, using the  
35  
36 well-known Langmuir-Blodgett (LB) film technique, can be used for further studies on the  
37  
38 microstructure of the mixed protein-lipid film; The microstructure of the film in the solid  
39  
40 support can then be imaged using electron microscopy<sup>24,25</sup> or atomic force microscopy  
41  
42 (AFM)<sup>26</sup>. For example, the former technique has been used to study the miscibility of  
43  
44 proteins and lipids at the air/water interface<sup>27</sup>. AFM has been used to study LB films (LB)  
45  
46 of a widely range of systems such as DPPC<sup>28</sup>, human proteins<sup>29</sup>, and mixtures of DPPC  
47  
48 with N-nitrosodiethylamine/bovine serum albumin<sup>30</sup>. Nevertheless, to the best of our  
49  
50  
51  
52  
53  
54  
55  
56  
57  
58  
59  
60

1  
2  
3 knowledge, neither microscope technique has been used for food protein monolayer  
4  
5 penetration studies.  
6

7  
8 In this work, we have studied the formation of 11S amaranth globulin monolayers on water  
9  
10 and buffer subphases and its interaction with L-DPPC in both subphases. In addition, the  
11  
12 comparison of the results obtained when L-DPPC monolayers were deposited on both  
13  
14 subphases is presented. The protein monolayers and its interaction with L-DPPC were done  
15  
16 in two different ways: i) direct deposition on the interface and ii) injecting the proteins  
17  
18 below the interface. Isotherm measurements and BAM observations along the compression  
19  
20 isotherm were performed to follow the pure protein behavior and its interaction with L-  
21  
22 DPPC. LB films were made to study the microstructure of the protein films and its mixture  
23  
24 with L-DPPC using AFM.  
25  
26  
27  
28  
29  
30  
31

## 32 **EXPERIMENTAL SECTION**

33  
34 **Protein extraction and purification, L-DPPC and subphases.** *Amaranthus*  
35  
36 *hypochondriacus* L. seeds, cv. Nutrisol were used for 11S globulin fraction isolation  
37  
38 according to Barba de la Rosa et. al.<sup>31</sup>. Briefly, suspensions of defatted flour/extracting  
39  
40 agents (1:10 w/v) were stirred for 1h at room temperature and centrifuged at 9000g for 20  
41  
42 min. In a sequential order; albumins were extracted with water, the precipitate was  
43  
44 resuspended in 10 mM phosphate buffer, 1 mM EDTA, pH=7.5, containing 0.1 M NaCl. A  
45  
46 second extraction was done with the same buffer and finally the pellet was wash with  
47  
48 deionized water. All supernatants were mixed together and named as 7S globulins. The  
49  
50 resulting precipitate was resuspended in 10 mM phosphate buffer, 1 mM EDTA pH 7.5  
51  
52 containing 0.8 M NaCl, a second extraction with the same buffer was done with the final  
53  
54  
55  
56  
57  
58  
59  
60

1  
2  
3 wash with water. The supernatant were mixed and named 11S globulins. Quantification of  
4 proteins was done using the protein Assay (BIO-RAD, Lab Hercules, CA USA).  
5

6  
7  
8 L-DPPC (1,2-Dihexadecanoyl-sn-glycero-3-phosphocholine,  $\geq 99\%$ ) was purchased from  
9 Sigma-Aldrich Inc, USA, and used without any further purification. L-DPPC was dissolved  
10 using chloroform (Sigma-Aldrich, USA  $\geq 99.99\%$ ) to prepare the spreading solution at a  
11 concentration 0.353 mg/ml. Ultrapure water (Nanopure-UV, Barnstead/Thermoline, 18.3  
12  $M\Omega\text{-cm}$  of resistivity) was used throughout all preparations.  
13  
14  
15  
16  
17  
18

19 **Langmuir monolayers, Langmuir-Blodgett films and BAM observations.** All  
20 monolayer isotherms and transferred LB films were prepared on a computerized Nima LB  
21 trough (601-BAM, Nima Technology Ltd., England) using a Wilhelmy plate to measure the  
22 lateral surface pressure,  $\Pi = \gamma^0 - \gamma$ . Temperature was kept constant at  $25 \pm 0.2$  °C with the  
23 aid of a water circulator bath (NESLAB, RTE-211, USA). The compression rate was 15  
24  $\text{cm}^2/\text{min}$ . All experiments were carried out in a dust-free environment room cleaned with a  
25 laminar flow hood. BAM observations were made along the isotherm measurements with a  
26 BAM I-ELLI 2000 (Nanofilm Technologies GmbH, Germany) apparatus, with a spatial  
27 resolution of ca. 2  $\mu\text{m}$ . The interface was illuminated at the water Brewster incidence angle  
28 ( $53.13^\circ$ ) for BAM observations and the analyzer was rotated for best contrast and to look  
29 for anisotropies of the film. The NIMA LB trough and BAM were placed together onto an  
30 optical table. The monolayers were transferred at a dipper speed of 1 mm/min in an upward  
31 stroke mode at a prefixed surface pressure. The mica was freshly cleaved just before the  
32 deposition. The AFM (see below) scanning was performed just after LB preparation.  
33  
34  
35  
36  
37  
38  
39  
40  
41  
42  
43  
44  
45  
46  
47  
48  
49  
50  
51  
52

53 **Globulin 11S films.** Two different methods were used to form globulin monolayers, in the  
54 first one, the protein was deposited with a microsyringe on a deionized water subphase or  
55  
56  
57  
58  
59  
60

1  
2  
3 buffer subphase, after 4 hrs the monolayer was compressed. In the second method the  
4  
5 protein was injected below the air/water or air/buffer subphases, in this case we waited 6  
6  
7 hrs. before compression, to allow protein diffusion and trapping by the surface.  
8  
9

10 **Monolayers of L-DPPC with globulin 11S.** Two methods to incorporate globulin 11S  
11  
12 into L-DPPC monolayer<sup>12</sup> were used. In the first one, the protein was deposited on the  
13  
14 subphase surface, water subphase or buffer subphase, drop-by-drop with the aid of a  
15  
16 microsyringe. After 15 min, 250  $\mu\text{L}$  of L-DPPC was deposited onto the surface, by  
17  
18 dropping it dissolved in the spreading solution. In the second method, L-DPPC was spread  
19  
20 on the subphase with the aid of a Hamilton microsyringe. We waited at least 20 min for  
21  
22 chloroform evaporation before monolayer compression, the barriers were closed a little and  
23  
24 the protein injected below the subphase surface passing a syringe into the bulk from the  
25  
26 outside part of the barriers, to disturb as a little as possible the L-DPPC monolayer, then the  
27  
28 barriers were fully opened again. After approximately 6 hrs, to allow protein diffusion to  
29  
30 the surface and to be able to obtain significant surface pressure for isotherm measurements,  
31  
32 the compression started. All experiments were repeated three times obtaining good  
33  
34 reproducibility within  $\pm 0.1$  mN/m.  
35  
36  
37  
38  
39

40 **AFM observations.** Transferred monolayer of both pure protein and its mixture with L-  
41  
42 DPPC were scanned with a NanoScope IIIa AFM (Digital Instruments, California, USA.)  
43  
44 with a J-scanner that has a maximum scanning area of  $100 \times 100 \mu\text{m}$ . We worked in  
45  
46 tapping mode to obtain topographic and deflection images, using  $\text{Si}_3\text{N}_4$  tips with a typical  
47  
48 force constant of  $0.3 \text{ Nm}^{-1}$ . 125  $\mu\text{m}$ -length tips with nominal resonance frequency of 300  
49  
50 kHz and spring constant of 40 N/m were used at room temperature in air. The oscillation  
51  
52 frequency for scanning was set 0.1-3 kHz below resonance. Low scan rates typically  
53  
54  
55  
56  
57  
58  
59  
60

1  
2  
3 between 0.5-1 Hz were used and the images were analyzed using the Digital Instruments  
4 software. AFM images were first obtained at low magnification and once a proper area was  
5 found, the scanning was changed to a higher resolution. Both height and deflection images  
6 were usually good enough. Therefore, the AFM images presented here are height images  
7 unless indicated otherwise.  
8  
9  
10  
11  
12  
13  
14  
15  
16  
17

## 18 **Results and Discussion**

19  
20 **L-DPPC monolayer.** Fig. 1 shows typical isotherms of L-DPPC monolayers at 25°C, on  
21 deionized water and on sodium phosphate buffer subphases. The isotherms on the buffered  
22 subphase are shifted slightly to higher surface pressures with respect those on water. These  
23 monolayers present two phase transitions; Gas-Liquid Expanded (G-LE) and LE-Liquid  
24 Condensed (LC)<sup>12</sup>. The G-LE coexistence is not shown. L-DPPC phase transitions onto a  
25 deionized water subphase have been widely studied, and one of the most interesting  
26 features is the formations of LC chiral three-arm domains in coexistence with the LE phase.  
27 BAM images show the characteristic three armed domains observed in L-DPPC Langmuir  
28 monolayer (see Figs. 1a and b)<sup>32</sup>. The shape of these domains depends on line tension,  
29 dipolar interaction and chiral contributions<sup>33</sup>. When we used a sodium phosphate buffered  
30 water subphase, BAM images didn't show the characteristic chiral domains, instead images  
31 show anisotropic domains, often with straight edges (see Figs. 1d and e). Similar  
32 observations on the shifting of isotherms to higher surface pressures and changes on  
33 domains morphology in monolayers of L-DPPC in the presence of different ions in the  
34 subphase have been reported<sup>34</sup>. They find that the LC phase is essentially unaffected by its  
35 interactions with the ions in the subphase while the LE phase is not. They propose that  
36  
37  
38  
39  
40  
41  
42  
43  
44  
45  
46  
47  
48  
49  
50  
51  
52  
53  
54  
55  
56  
57  
58  
59  
60

1  
2  
3 changes in domain morphology are probably due to an entropic stabilization of the LE  
4 phase. We believe that this stabilization must change the LC-LE line tension, thus  
5 preventing the formation of chiral patterns. In addition, we can argue that this stabilization  
6 will made the LE phase more robust, which shift the L-DPPC isotherm to higher surface  
7 pressures, as observed experimentally. The LE-LC transition was characterized by  
8 coalescence of the LC domains on further compression, to make a uniform film on both  
9 subphases (see Figs. 1c and f). L-DPPC monolayer on deionized water subphase collapse at  
10  $\Pi \sim 44.5$  mN/m and  $A \sim 41 \text{ \AA}^2/\text{molecule}$ , while in the phosphate buffer subphase the  
11 collapse occurs at  $\Pi \sim 41.5$  mN/m and  $A \sim 42 \text{ \AA}^2/\text{molecule}$ .

12  
13  
14  
15  
16  
17  
18  
19  
20  
21  
22  
23  
24  
25 **Globulin 11S Langmuir films.** As it is explained below, isotherms indicate that 11S  
26 protein from amaranth seed can be adsorbed at the air/water and air/buffer interfaces.  
27 Isotherms where the protein solution was directly deposited at the air/water interface,  $T =$   
28  $25^\circ \text{ C}$ , show a high amount of molecules trapped on the interface and it is reflected with a  
29 rapid increase in surface pressure upon compression, see Fig. 2. Isotherms on both  
30 subphases are qualitatively different despite its closeness, especially at the lower surface  
31 pressures. The isotherm of globulin 11S on a water subphase shows a small shoulder, which  
32 in lipid monolayers, such as phospholipids, would be indicative of a phase transition.  
33 However, this is not the case for the protein films since BAM observations did not give us  
34 any indication of a phase transition. In the case of the isotherm of globulin 11S on the  
35 buffer subphase, it shows a continuous increase with some light slope changes, but again,  
36 BAM observations did not show any phase transition; isotherms show breaks that might  
37 indicate some phase transitions, BAM observations ruled out any transitions since no  
38 coexistence or phase changes were observed, this is only a homogeneous film was observed  
39  
40  
41  
42  
43  
44  
45  
46  
47  
48  
49  
50  
51  
52  
53  
54  
55  
56  
57  
58  
59  
60

1  
2  
3 along the isotherms up to collapse (see Fig. 2). Furthermore, isotherms taken at 3, 4 and 6  
4  
5 hrs after depositing the protein on the surface were quite reproducible. This might indicate  
6  
7 that the amount of protein trapped by the interface is constant in the time frame of the  
8  
9 experiments. However, we think that not all the protein deposited was trapped by the  
10  
11 interface. In the case of the water subphase, since the protein is not water soluble, the  
12  
13 amount that went into the bulk might have aggregated and precipitated. This was  
14  
15 corroborated after finishing the experiments and cleaning the bottom surface of the trough,  
16  
17 where a good amount of protein was found on it. This protein precipitation was not  
18  
19 observed when the buffer subphase was used, therefore we believe that the protein film  
20  
21 trapped at the interface did not change much, because either the protein that went into the  
22  
23 buffer subphase diffused slowly towards the interface, not changing the protein surface  
24  
25 concentration, or the monolayers acted as a Gibbs monolayer, reaching an equilibrium  
26  
27 concentration at the interface within the time frame of the experiments.  
28  
29  
30  
31  
32

33  
34 Isotherms indicate that the monolayer of protein deposited on water suffered fracture  
35  
36 collapse at  $\Pi \sim 39$  mN/m, but BAM observations indicated that continuous collapse  
37  
38 occurred at lower surface pressures. Fracture collapse of the isotherm of globulin deposited  
39  
40 on buffer occurs at higher surface pressures,  $\Pi \sim 44$  mN/m, but continuous collapse also  
41  
42 occurred at lower surface pressures as indicated by BAM observations. In general, BAM  
43  
44 observations (Figs. 2a, 2b, 2d, 2e), showed that during monolayer compression only a  
45  
46 homogenous phase with small three-dimensional aggregates was observed. However,  
47  
48 continuous collapse was present at pressures over  $\Pi > 15$  mN/m, defined by the formation  
49  
50 of a high number of large three-dimensional aggregates and structures, see Figs. 2c and 2f,  
51  
52 where the white structures are much thicker than the rest of the film. This collapse behavior  
53  
54  
55  
56  
57  
58  
59  
60

1  
2  
3 already had been observed in globulin 11S of soy seed films, under similar experimental  
4 conditions<sup>35</sup>.  
5  
6

7  
8 Fig. 3 shows the results when the amaranth 11S globulins were injected under the two  
9 working interfaces. Compression started six hours after injecting the sample. Isotherms and  
10 BAM observations in deionized water subphase showed that at low surface pressures a  
11 phase coexistence region between two fluid phases is present; the dark area would  
12 correspond to a Gas (G) phase and the white structures (2-D soap-froth and rounded  
13 domain structures) would correspond to a Liquid Expanded (LE) like phase (see Fig. 3a and  
14 b). The surface pressure was quite low during most of the compression, which can be  
15 attributed to the presence of the two-dimensional (2D) G phase. In this case a 2D G phase  
16 means a phase with low density of protein molecules (or regions of almost bare water). The  
17 protein was injected in the bulk a few millimeters from the surface and then a small amount  
18 of protein diffused towards the surface. Since globulins are not water soluble, probably  
19 most of the protein aggregated and precipitated to the bottom of the trough, for that reason  
20 the lateral pressure does not increase much upon compression. After removing the  
21 subphase, indeed precipitated protein was found on the bottom of the trough, as a protein  
22 film. BAM images show the existence of rings and soap-froths (see Figs. 3a and b) similar  
23 to those observed in colloidal systems<sup>36</sup>. At higher surface pressures, BAM images showed  
24 that the amaranth globulin 11S film was in a homogeneous condensed phase with few small  
25 3D aggregates (Fig. 3c). It is worth noticing that in this case, the amount of protein trapped  
26 at the air/water interface was lower than the amount of protein trapped at air/water interface  
27 when the globulin was directly spread on the surface.  
28  
29

30  
31  
32  
33  
34  
35  
36  
37  
38  
39  
40  
41  
42  
43  
44  
45  
46  
47  
48  
49  
50  
51  
52  
53  
54  
55  
56  
57  
58  
59  
60  
61  
62  
63  
64  
65  
66  
67  
68  
69  
70  
71  
72  
73  
74  
75  
76  
77  
78  
79  
80  
81  
82  
83  
84  
85  
86  
87  
88  
89  
90  
91  
92  
93  
94  
95  
96  
97  
98  
99  
100  
101  
102  
103  
104  
105  
106  
107  
108  
109  
110  
111  
112  
113  
114  
115  
116  
117  
118  
119  
120  
121  
122  
123  
124  
125  
126  
127  
128  
129  
130  
131  
132  
133  
134  
135  
136  
137  
138  
139  
140  
141  
142  
143  
144  
145  
146  
147  
148  
149  
150  
151  
152  
153  
154  
155  
156  
157  
158  
159  
160  
161  
162  
163  
164  
165  
166  
167  
168  
169  
170  
171  
172  
173  
174  
175  
176  
177  
178  
179  
180  
181  
182  
183  
184  
185  
186  
187  
188  
189  
190  
191  
192  
193  
194  
195  
196  
197  
198  
199  
200  
201  
202  
203  
204  
205  
206  
207  
208  
209  
210  
211  
212  
213  
214  
215  
216  
217  
218  
219  
220  
221  
222  
223  
224  
225  
226  
227  
228  
229  
230  
231  
232  
233  
234  
235  
236  
237  
238  
239  
240  
241  
242  
243  
244  
245  
246  
247  
248  
249  
250  
251  
252  
253  
254  
255  
256  
257  
258  
259  
260  
261  
262  
263  
264  
265  
266  
267  
268  
269  
270  
271  
272  
273  
274  
275  
276  
277  
278  
279  
280  
281  
282  
283  
284  
285  
286  
287  
288  
289  
290  
291  
292  
293  
294  
295  
296  
297  
298  
299  
300  
301  
302  
303  
304  
305  
306  
307  
308  
309  
310  
311  
312  
313  
314  
315  
316  
317  
318  
319  
320  
321  
322  
323  
324  
325  
326  
327  
328  
329  
330  
331  
332  
333  
334  
335  
336  
337  
338  
339  
340  
341  
342  
343  
344  
345  
346  
347  
348  
349  
350  
351  
352  
353  
354  
355  
356  
357  
358  
359  
360  
361  
362  
363  
364  
365  
366  
367  
368  
369  
370  
371  
372  
373  
374  
375  
376  
377  
378  
379  
380  
381  
382  
383  
384  
385  
386  
387  
388  
389  
390  
391  
392  
393  
394  
395  
396  
397  
398  
399  
400  
401  
402  
403  
404  
405  
406  
407  
408  
409  
410  
411  
412  
413  
414  
415  
416  
417  
418  
419  
420  
421  
422  
423  
424  
425  
426  
427  
428  
429  
430  
431  
432  
433  
434  
435  
436  
437  
438  
439  
440  
441  
442  
443  
444  
445  
446  
447  
448  
449  
450  
451  
452  
453  
454  
455  
456  
457  
458  
459  
460  
461  
462  
463  
464  
465  
466  
467  
468  
469  
470  
471  
472  
473  
474  
475  
476  
477  
478  
479  
480  
481  
482  
483  
484  
485  
486  
487  
488  
489  
490  
491  
492  
493  
494  
495  
496  
497  
498  
499  
500  
501  
502  
503  
504  
505  
506  
507  
508  
509  
510  
511  
512  
513  
514  
515  
516  
517  
518  
519  
520  
521  
522  
523  
524  
525  
526  
527  
528  
529  
530  
531  
532  
533  
534  
535  
536  
537  
538  
539  
540  
541  
542  
543  
544  
545  
546  
547  
548  
549  
550  
551  
552  
553  
554  
555  
556  
557  
558  
559  
560  
561  
562  
563  
564  
565  
566  
567  
568  
569  
570  
571  
572  
573  
574  
575  
576  
577  
578  
579  
580  
581  
582  
583  
584  
585  
586  
587  
588  
589  
590  
591  
592  
593  
594  
595  
596  
597  
598  
599  
600  
601  
602  
603  
604  
605  
606  
607  
608  
609  
610  
611  
612  
613  
614  
615  
616  
617  
618  
619  
620  
621  
622  
623  
624  
625  
626  
627  
628  
629  
630  
631  
632  
633  
634  
635  
636  
637  
638  
639  
640  
641  
642  
643  
644  
645  
646  
647  
648  
649  
650  
651  
652  
653  
654  
655  
656  
657  
658  
659  
660  
661  
662  
663  
664  
665  
666  
667  
668  
669  
670  
671  
672  
673  
674  
675  
676  
677  
678  
679  
680  
681  
682  
683  
684  
685  
686  
687  
688  
689  
690  
691  
692  
693  
694  
695  
696  
697  
698  
699  
700  
701  
702  
703  
704  
705  
706  
707  
708  
709  
710  
711  
712  
713  
714  
715  
716  
717  
718  
719  
720  
721  
722  
723  
724  
725  
726  
727  
728  
729  
730  
731  
732  
733  
734  
735  
736  
737  
738  
739  
740  
741  
742  
743  
744  
745  
746  
747  
748  
749  
750  
751  
752  
753  
754  
755  
756  
757  
758  
759  
760  
761  
762  
763  
764  
765  
766  
767  
768  
769  
770  
771  
772  
773  
774  
775  
776  
777  
778  
779  
780  
781  
782  
783  
784  
785  
786  
787  
788  
789  
790  
791  
792  
793  
794  
795  
796  
797  
798  
799  
800  
801  
802  
803  
804  
805  
806  
807  
808  
809  
810  
811  
812  
813  
814  
815  
816  
817  
818  
819  
820  
821  
822  
823  
824  
825  
826  
827  
828  
829  
830  
831  
832  
833  
834  
835  
836  
837  
838  
839  
840  
841  
842  
843  
844  
845  
846  
847  
848  
849  
850  
851  
852  
853  
854  
855  
856  
857  
858  
859  
860  
861  
862  
863  
864  
865  
866  
867  
868  
869  
870  
871  
872  
873  
874  
875  
876  
877  
878  
879  
880  
881  
882  
883  
884  
885  
886  
887  
888  
889  
890  
891  
892  
893  
894  
895  
896  
897  
898  
899  
900  
901  
902  
903  
904  
905  
906  
907  
908  
909  
910  
911  
912  
913  
914  
915  
916  
917  
918  
919  
920  
921  
922  
923  
924  
925  
926  
927  
928  
929  
930  
931  
932  
933  
934  
935  
936  
937  
938  
939  
940  
941  
942  
943  
944  
945  
946  
947  
948  
949  
950  
951  
952  
953  
954  
955  
956  
957  
958  
959  
960  
961  
962  
963  
964  
965  
966  
967  
968  
969  
970  
971  
972  
973  
974  
975  
976  
977  
978  
979  
980  
981  
982  
983  
984  
985  
986  
987  
988  
989  
990  
991  
992  
993  
994  
995  
996  
997  
998  
999  
1000

1  
2  
3 (see Figs. 2 and 3). Therefore, the lateral pressure obtained in the protein sample injected in  
4  
5 buffer is greater than that obtained if the protein was injected in a deionized water  
6  
7 subphase, as it can be observed in Fig. 3. This indicates that a greater amount of protein  
8  
9 diffuses towards the buffer surface and gets trapped. This different behavior might be due  
10  
11 to the high solubility of the globulin in the phosphate buffer, which allows the transport of  
12  
13 the protein in a more effective way, without aggregation and further precipitation. BAM  
14  
15 observations showed that there weren't changes along the isotherm; this is, there is always  
16  
17 a homogeneous and continuous protein monolayer, with a scarce number of 3-D aggregates  
18  
19 (see Figure 3c, 3d y 3e).  
20  
21  
22  
23  
24  
25  
26

### 27 **Mixed films of Globulin 11S and L-DPPC**

28  
29 Fig. 4 shows the experiments where L-DPPC was spread on amaranth globulin 11S film at  
30  
31 the air/water and air/buffer subphases.  $\Pi$ -A isotherms for the mixed films in both cases  
32  
33 show a rapid increase in surface pressure upon compression, indicating that there must be a  
34  
35 continuous mixed film at the interface; this is, only condensed phases are present. The  
36  
37 protein presence causes the disappearance of the coexistence region of the characteristic  
38  
39 LE-LC phases in L-DPPC isotherm monolayers. In this case, we performed experiments  
40  
41 with waiting times before compression of 4, 6 and 8 hrs after deposition of the L-DPPC and  
42  
43 isotherms were essentially reproducible within  $\pm 1$  mN/m.  
44  
45  
46  
47

48 Fig. 4a shows a BAM image at low pressures, c. a.  $\Pi \sim 0$  mN/m, of the film on water  
49  
50 subphase. On the top left corner of the image, one can observe a large domain that shows a  
51  
52 bright fingering instability. The rest of Fig. 4a shows the formation of some small rounded  
53  
54 domains, often connected, which show typical internal anisotropy due to molecular tilting.  
55  
56  
57  
58  
59  
60

1  
2  
3 Since globulin protein molecules are rounded when folded or disorganized when unfolded,  
4 domains with internal anisotropic structure must be formed mostly by L-DPPC molecules.  
5  
6 Therefore, we proposed that upon compression, L-DPPC start being expelled from the  
7  
8 mixed film like that located on top left corner of the image. We recognized this waving  
9  
10 instability as Mullins-Sekerka instability due to the expelling of the L-DPPC molecules  
11  
12 from the mixed film. The Mullins-Sekerka instability is associated with the mass transport  
13  
14 throughout interfaces due to concentration gradients in mixtures, i.e. with the expulsion of  
15  
16 impurities of a phase rich in one of the components, in this case the L-DPPC small  
17  
18 molecules being expelled from the protein rich phase. In addition, we ruled out the presence  
19  
20 of a G phase because the isotherm increases its surface pressure rapidly after compression.  
21  
22 Therefore, the rounded domains, with internal anisotropy, must correspond to the L-DPPC  
23  
24 LC phase while the continuous darker phase surrounding the small domains must  
25  
26 correspond to the L-DPPC LE phase.  
27  
28  
29  
30  
31  
32

33  
34 Fig. 4b shows regions with mostly L-DPPC phases, where the LC domains start to coalesce  
35  
36 and the area covered by the LE phase becomes smaller. Remarkably, separation between  
37  
38 protein rich and LC L-DPPC rich regions is completed at higher surface pressures. Fig. 4c  
39  
40 shows a typical image of these large regions; since the protein molecules are bulkier and  
41  
42 thicker than the phospholipid molecules, we assign the brighter regions as protein-rich  
43  
44 regions and the dark regions as L-DPPC LC-rich regions. The large protein-rich regions  
45  
46 show remnants of the Mullins-Sekerka instability along its interface with the L-DPPC rich  
47  
48 region.  
49  
50  
51

52  
53 On the other hand, when L-DPPC was spread on the protein film supported on the buffer  
54  
55 subphase, we observed the formation of a mostly continuous film at low surface pressure  
56  
57 (see Fig. 4d). The film formed is a rather a good mixture of both amaranth globulin 11S  
58  
59  
60

1  
2  
3 protein and L-DPPC. However, at intermediate surface pressures, c.a. 15 mN/m, we  
4  
5 observed again the separation of protein- and L-DPPC-rich regions as shown in Fig. 4e, but  
6  
7 in this case no Mullins-Sekerka instability was observed. The thicker large gray island on  
8  
9 the top of this image corresponds to the protein-rich region while the dark region must be  
10  
11 the L-DPPC LC-rich region. The protein-rich island contains imbedded some large white  
12  
13 areas that are elongated in the same direction. Not capture by the still images, is the relative  
14  
15 movement of the protein-rich island and the L-DPPC region. Since the amaranth globulin  
16  
17 11S is more stable in buffer than in water, i. e. it retains its three dimensional globular  
18  
19 shape, our observations lead us to propose that the protein-rich island acts like an ultrathin  
20  
21 granular film rather than a condensed compact region; this is, the island is like a two-  
22  
23 dimensional granular fluid. Thus the island relative movement produces shearing,  
24  
25 elongating the white domains within it in the shearing direction. The granular nature of  
26  
27 domains was corroborated by AFM observations, as discussed below. Furthermore, Fig. 4f  
28  
29 shows clearly domains of protein-rich (whitest domain), mixed domains (granular grey  
30  
31 region) and L-DPPC-rich region (dark region). Again, no instability was observed at the  
32  
33 border of the protein-rich and L-DPPC-rich interface. However, the mixed region shows  
34  
35 patterns that resemble spinodal decomposition or a microphase separation, indicating the  
36  
37 separation of the protein and lipid molecules. The lack of an instability at the border of the  
38  
39 protein-rich regions in the experiments on a buffer subphase, indicates that the separation  
40  
41 mechanism differs from that on the water subphase. It is possible that the differences arise  
42  
43 because the protein on the buffer subphase acts more like a granular material while on the  
44  
45 water subphase might be acting like a melt due to its tendency to unfold in water.  
46  
47  
48  
49  
50  
51  
52  
53

54  
55 Fig. 5 shows isotherms and BAM images when a globulin 11S solution was injected  
56  
57 beneath the preformed L-DPPC monolayer at deionized water and buffer surfaces.  
58  
59  
60

1  
2  
3 Compression started  $\sim 4$  hrs after the protein was injected. The surface pressure in both  
4 isotherms started to rise as soon as the systems were compressed, and no flat LC-LE  
5 coexistence region of L-DPPC (see Fig. 1) was observed. Both isotherms are very similar  
6 up to about 4 mN/m and 85  $\text{\AA}^2/\text{molecule}$ , where the isotherm obtained on the water  
7 subphase becomes more compressible up to about 10 mN/m and 60  $\text{\AA}^2/\text{molecule}$ , after  
8 which the situation reverses and the film becomes less compressible than the one obtained  
9 on the buffer surface. Finally, the pressure readings of the isotherm obtained on the water  
10 surface surpass those of the isotherm obtained on the buffer surface at about 17 mN/m and  
11 50  $\text{\AA}^2/\text{molecule}$ . In both subphases, BAM images show the presence of small domains of  
12 the protein/L-DPPC mixture at low surface pressures, as shown in Figs. 5a and d. The L-  
13 DPPC LC domains on the water subphase are somewhat bigger, and with small instabilities  
14 at the borders, than those observed on the buffer subphase that show a more stable straight  
15 borders, similar to those observed without protein (see Figs. 1d-e). In addition, domains  
16 show internal tilting anisotropy, which indicates that they are made mostly by L-DPPC  
17 molecules and correspond to the LC phase. Thus the continuous dark areas must also  
18 correspond to the phospholipid LE phase.

19  
20  
21  
22  
23  
24  
25  
26  
27  
28  
29  
30  
31  
32  
33  
34  
35  
36  
37  
38  
39  
40  
41  
42  
43  
44  
45  
46  
47  
48  
49  
50  
51  
52  
53  
54  
55  
56  
57  
58  
59  
60  
At low surface pressures, BAM images gave little evidence of the presence of the globulin  
11S on the L-DPPC monolayer. However, with further compression, c. a.  $\Pi > 15\text{mN/m}$ , the  
LC domains grow further at the expense of the LE phase and some white dots become  
evident. We think that these white dots are evidence of the protein presence. Furthermore,  
the instabilities in the LC domains on the water surface become larger and LC domains  
observed at the buffer subphase start to developed small instabilities (clearly observed at  
high magnification). We proposed again that they are Mullins-Sekerka instabilities, but in  
these cases the protein molecules are being expelled from the LC phospholipid domains.

1  
2  
3 The instabilities are larger in the LC domains at the water surface because they contain a  
4 higher concentration of protein than the LC domains obtained in buffer, since ions stabilize  
5 the LE phase, as discussed above, making difficult the protein penetration/interaction with  
6 the LE phase of the monolayer in the latter case.  
7  
8  
9

10  
11  
12 At higher surface pressure, we found evidence of protein monolayer inside of the LC  
13 domains as well as at the LC-LE interface in the experiments on the water subphase. It is  
14 strange that almost no evidence of protein is observed in the LE phase. It is possible that in  
15 this case the protein is unfolded, making it difficult to distinguish from the L-DPPC LE  
16 phase. However, the protein is almost entirely located at the LC-LE interface in the  
17 experiments done on buffer. In general, we believe that more protein penetrates/interacts  
18 with the L-DPPC monolayer on water than on buffer. These facts and assumptions would  
19 explain the different behavior of the isotherms of Fig. 5; at the beginning the monolayer on  
20 buffer is slightly more rigid than that on water, due to buffer ion stabilization of the LE  
21 phase, making it less compressible. This stabilization also prevents the  
22 penetration/interaction with the globulin having more protein molecules in the experiments  
23 on water than in the experiments on buffer. Therefore, the compressibility changes midway  
24 the compression process, because on water we will have more total number of molecules at  
25 the interface than on buffer.  
26  
27  
28  
29  
30  
31  
32  
33  
34  
35  
36  
37  
38  
39  
40  
41  
42  
43  
44  
45  
46  
47

#### 48 **AFM Results.**

49  
50 Langmuir-Blodgett films were prepared for each one of the different experiments for  
51 further analysis by AFM. For completeness of the present work, we also present the case  
52 when pure L-DPPC was deposited on a deionized water or a buffer subphase, the transfer  
53 process was done at a lateral pressure of  $\Pi=14$  mN/m. This pressure was chosen above the  
54  
55  
56  
57  
58  
59  
60

1  
2  
3 LC-LE transition, as BAM images show that the L-DPPC Langmuir monolayer on both  
4 subphases is in the pure LC phase. At this pressure, the characteristic LC domains have  
5  
6  
7  
8  
9  
10  
11  
12  
13  
14  
15  
16  
17  
18  
19  
20  
21  
22  
23  
24  
25  
26  
27  
28  
29  
30  
31  
32  
33  
34  
35  
36  
37  
38  
39  
40  
41  
42  
43  
44  
45  
46  
47  
48  
49  
50  
51  
52  
53  
54  
55  
56  
57  
58  
59  
60

LC-LE transition, as BAM images show that the L-DPPC Langmuir monolayer on both subphases is in the pure LC phase. At this pressure, the characteristic LC domains have coalesced, forming a uniform phase, with only defect lines and small holes remnant of the LE phase, as shown in Fig. 6: These holes and lines could not be observed by BAM because they are beyond its resolution. Fig. 6a show a flat film with a high of  $\approx 2.8$  nm with respect to the mica surface, but also reveal the presence of curved lines of smaller height,  $z \approx 2.3$  nm; these lines could correspond to the union (healing lines) between two or more chiral LC domains. L-DPPC molecules have a size of  $\approx 3$  nm, therefore we can assume that the thicker flat and continuous phase correspond to LC phase while the darker lines correspond to a metastable remnant of the LE phase. AFM images for the monolayer spread on a buffer subphase (see Fig. 6b) show that the healing lines are not curvy as those of Fig. 6a. This is in good agreement with BAM observations which show that on a water buffer the LC domains are chiral, while those on the buffer subphase are not. We observed an unusually large relative difference in height between the LE and LC phase of the film of about 1 nm, while on water this height difference is about 0.5 nm. This LC-LE height difference might be explained as follows: The LC phase of L-DPPC on buffer does not produce chiral structures, therefore it might have a lower tilt angle than the LC phase that produces chiral structures on deionized water. In addition, the buffer ions might only penetrate the LE phase but not the LC phase<sup>34</sup>, since the phosphate ions are rather large, the L-DPPC molecules will be more separated from each other in the LE phase on buffer than on water, giving the aliphatic chains more room to sample more configurations, thus making the LE phase thinner on average, increasing the height difference between the LC to LE phases on buffer with respect to the same phases on water.

1  
2  
3 Fig. 7 presents the images of globulin 11S transferred from both water and buffer at  $\Pi \sim 18$   
4 mN/m. Two aspects are immediately observed, one is that the films is not a monolayer,  
5 since many aggregates are formed, and the second is that those aggregates are globular.  
6  
7 However, the globules formed on water are somewhat bigger than those globules formed on  
8 buffer, clearly confirming the tendency of globulin 11S to aggregate in water, while the  
9 phosphate buffer tends to stabilize the individual proteins. Most of the protein aggregates  
10 on water lie in the size range between 50 to 70 nm (see Figs. 7a-b). Figs. 7c-d show images  
11 of globulin 11S deposited on buffer. It was noticed that they form smaller globular  
12 structures than the sample deposited on water. The sizes of these globules range between 25  
13 to 50 nm. The sizes of the smaller globules might correspond to the actual protein size, thus  
14 it is clear from the images that the buffer does really gets the protein dispersed and avoid its  
15 aggregation. In general, globular structures were expected given the rounded nature of  
16 globulin 11S.  
17  
18  
19  
20  
21  
22  
23  
24  
25  
26  
27  
28  
29  
30  
31  
32

33  
34 AFM images when globulin 11S was injected below the interface and transferred at  $\Pi \sim 8$   
35 mN/m are presented in Fig. 8. Note that in the film transferred from the air/water interface  
36 the globular structures are scarce, this is a smooth film was observed as shown in Figs. 8a  
37 and b instead of the globular structures shown in Fig. 7. It is possible that the protein is  
38 unfolded in a deionized water subphase, therefore when it is trapped by the interface  
39 proteins formed a two-dimensional fluid- or melt-like film. On the other hand, films  
40 extracted when the globulin was injected below the air/buffer interface and allowed to  
41 diffuse to the interface, showed mostly a dense monolayer formed by globular protein  
42 structures, see Figs. 8c and d, i.e. the protein is not unfolded. Interestingly enough, the film  
43 is highly ordered, with crystal-like two-dimensional order: the inset in Fig. 8d is the Fourier  
44  
45  
46  
47  
48  
49  
50  
51  
52  
53  
54  
55  
56  
57  
58  
59  
60

1  
2  
3 transform of the image, which qualitatively shows a good order of the protein monolayer.  
4  
5 The monolayer contains defects in the form of small three-dimensional aggregates (white  
6  
7 dots) and vacancies, however. The present of these defects might explain the high  
8  
9 compressibility of the monolayer observed in the isotherm, see Fig. 3. Nevertheless, our  
10  
11 results show that one can build well ordered, two-dimensional crystal-like structures out of  
12  
13 globular proteins, similar to those formed with metallic nanoparticles<sup>37</sup>, which can have  
14  
15 potential applications in technology, such as molecular electronics.  
16  
17

18  
19 Fig. 9 show images obtained when globulin 11S was deposited on air/water or air/buffer  
20  
21 interfaces and immediately a L-DPPC solution was spread on it. When the protein was  
22  
23 deposited on a deionized water subphase, Figs. 9a)-c), it is clearly observed the formation  
24  
25 of coexistence regions; protein- and L-DPPC-rich regions; the small-rounded domains and  
26  
27 the large domain at the bottom of the image correspond to protein-rich regions, where one  
28  
29 can easily observe that protein globules are the main structures of these domains. The  
30  
31 rounded domains are surrounded by a continuous, shallower phase that contains a good  
32  
33 number of globular protein structures, but from the height of the majority phase we identify  
34  
35 it as composed mainly of L-DPPC molecules. Fig. 9c) is a close up image of one of the  
36  
37 protein-rich domains, typically these domains shows wiggles at their borders, reminiscent  
38  
39 of an instability, probably due to the expelling of L-DPPC molecules from their interior  
40  
41 upon compression, in agreement with BAM observations (see above). In addition, the  
42  
43 protein-rich phase shows the formation of holes that are discussed below. Figs 9d)-f) shows  
44  
45 the mixture on buffer subphase. The AFM images show a fracture film; apparently L-DPPC  
46  
47 forms fractal-like channels in the protein-DPPC mixture that percolates the image. In  
48  
49 addition, in this percolated phase one can distinguish globules embedded in a continuous  
50  
51 lipid film and the formation of three dimensional aggregates. We believe that these fractal-  
52  
53  
54  
55  
56  
57  
58  
59  
60

1  
2  
3 like channels help the DPPC molecules to move out of the protein-rich domains during  
4  
5 compression, thus avoiding the formation of Mullins-Sekerka instabilities at the protein-  
6  
7 and DPPC-rich domains interface. Furthermore, these channels will also make these  
8  
9 protein-rich domains labile against stress forces, making act as a two-dimensional liquid or  
10  
11 granular film, in agreement with BAM observations discussed above.  
12  
13

14  
15 In addition, large protein-rich domains like the one at the bottom of Figs. 9a) and b), show a  
16  
17 remarkable internal nanohole structure: Fig. 10 shows a typical higher magnification  
18  
19 obtained from these large protein-rich regions, in which we can observe the presence of  
20  
21 aggregates with a hole at the center. These aggregates have an average size of  $22.38 \pm 1.55$   
22  
23 nm and the average size of holes is  $8.1 \pm 1.19$  nm. It is believe that this kind of proteins  
24  
25 form channels *in vivo* for water transport during seed germination, and therefore, the  
26  
27 presence of holes in mixtures of this protein with DPPC might evidence its tendency for  
28  
29 channel formation.  
30  
31  
32

33  
34 Finally, we show the images obtained by AFM of the experiments in which the protein was  
35  
36 injected below a L-DPPC monolayer; the monolayer was deposited on a deionized water or  
37  
38 on buffer subphases, see Fig. 11. The images 11a-c correspond to the case of a water sub-  
39  
40 phase, for which we waited 6 hr before compression to a given surface pressure for LB  
41  
42 transfer; in order for the globulin to penetrate or interact with the L-DPPC film. In images  
43  
44 11a-b, we observed the presence of small aggregates that form short fibril structures. On  
45  
46 higher magnification of the image, we observed that the aggregates that form fibers were  
47  
48 united by a continuous shallower phase than the aggregates, possibly unfolded protein,  
49  
50 which can be clearly observed in image 11c. In this case, due to the properties of the  
51  
52  
53  
54  
55  
56  
57  
58  
59  
60

1  
2  
3 globulins in water, the continuous phase could be a mixture of unfolded protein and DPPC,  
4  
5 but no clear evidence of DPPC-rich domains was found.  
6  
7

8 A very different behavior was observed when a buffer subphase was used; no fiber  
9  
10 formation was observed. In addition, large domains that appear quite flat corresponding to  
11  
12 the LC phase of L-DPPC were observed, although the height average of these domains is of  
13  
14 approximately 6 nm, which is approximately twice those of L-DPPC monolayer, indicating  
15  
16 that they correspond to a bilayer. Therefore, this bilayer must onto top a monolayer, with  
17  
18 the hydrophobic tails of the top layer directed towards the air. Furthermore, the LC domains  
19  
20 of the bilayer are irregular and much less protein globules are evident even in the  
21  
22 monolayer regions. This behavior, at the transfer pressure of 18 mN/m, is in agreement  
23  
24 with isotherm and BAM observations, which show limited presence of proteins with the L-  
25  
26 DPPC monolayer.  
27  
28  
29  
30  
31  
32  
33

### 34 CONCLUSIONS

35  
36 In this work, we show that pure globulin 11S proteins form films on the surface of  
37  
38 deionized water and of buffer subphases. Two different methods were used to test protein  
39  
40 film formation: the first one was direct depositing of the protein on the surface and the  
41  
42 second was by injecting it on the subphase below the surface. The first method produced  
43  
44 globular aggregates of the protein, although the globules formed in buffer were mostly of  
45  
46 molecular size. The second method, however, produced very different results: isotherms in  
47  
48 deionized water show a much less amount of globular structures than in buffer. In addition,  
49  
50 AFM images showed that in water the protein might have unfolded, forming a smooth film,  
51  
52 while in buffer the protein formed a remarkably, well organized, crystalline-like two-  
53  
54 dimensional film. This later organization must be due to the globular nature of the protein,  
55  
56  
57  
58  
59  
60

1  
2  
3 which in buffer behaves as a nanoparticle. In fact, such type of organization has been  
4 shown in colloidal systems<sup>36</sup> and metal nanoparticles<sup>37</sup> at the air/water interface. Therefore,  
5  
6 our procedure can be used to prepared well organized or even crystalline-like films of  
7  
8 globular proteins, which can be used for protein crystal structure analysis or for  
9  
10 technological application based on well-organized protein arrays.  
11  
12

13  
14 On the other hand, when an L-DPPC film is deposited on a globulin film, the isotherm  
15  
16 behavior is similar on both subphases, but at higher surface pressure the L-DDPC is  
17  
18 squeeze out forming protein- and L-DPPC-rich domains; while L-DPPC is squeeze out,  
19  
20 Mullins-Sekerka instabilities are formed at the edge of the domains in experiments on  
21  
22 water. Therefore, the experiments indicate that protein-lipid mixture should not be used at  
23  
24 relatively high pressure, because they might separate. Furthermore, AFM observations  
25  
26 revealed that the protein-rich domains formed nanoholes, which might be taken as an  
27  
28 indication of the natural tendency of the protein mixture with lipids to form such structures,  
29  
30 which might also have some implications for water transport *in vivo* during seed  
31  
32 germination.  
33  
34

35  
36 When the L-DPPC Langmuir monolayer is first formed and the protein is injected in the  
37  
38 subphase, BAM observation revealed little penetration of the protein, even in the LE phase.  
39  
40 At higher compressions, the protein seems to accumulate at the LE-LC interface in both  
41  
42 subphases. AFM images confirmed these observations, but it seems that there is more  
43  
44 protein penetration in water than in buffer. This difference can be understood because of the  
45  
46 increased stability of the L-DPPC Langmuir monolayer by the buffer ions, decreasing the  
47  
48 protein penetration. Furthermore, the protein-L-DPPC mixture seems to develop small  
49  
50 fiber-like structures on water; fiber formation is very important in the food industry, and  
51  
52  
53  
54  
55  
56  
57  
58  
59  
60

our experiments suggests that amaranth 11S globulin could make textures similar to globulin 11S from soybean<sup>38</sup>.

Acknowledgements. This work was supported by CONACYT Grants 60833, PIFI-PROMEP and UASLP-FAI. ALFV would like to acknowledge CONACYT for postdoctoral support.

## REFERENCES

- (1) Möhwald, H. *Ann. Rev. Phys. Chem.* **1990**, *41*, 441.
- (2) Rodríguez Patino, J. M.; Carrera Sánchez, C.; Molina Ortiz, S. E.; Rodríguez Niño, M. R.; Añón, M. C. *Ind. Eng. Chem. Res.* **2004**, *43*, 1681.
- (3) Miñones Conde, J.; Miñones Trillo, J.; Rodríguez Patino, J. M. *J. Phys. Chem. B* **2006**, *110*, 1152.
- (4) Kamilya, T.; Pal, P.; Talapatra, G. B. *J. Phys. Chem. B* **2007**, *111*, 1199.
- (5) Fainerman, V.B.; Zhao, J.; Vollhardt, D.; Malievski, A.V.; Li, J. B. *J. Phys. Chem. B* **1999**, *103*, 8998.
- (6) Cornell, D. G.; Patterson, D. L. *J. Agric. Food. Chem.* **1989**, *37*, 1455.
- (7) Rodríguez-Patino, J. M.; Carrera-Sánchez, C.; Cejudo-Fernández, M.; Rodríguez-Niño, M. R. *J. Phys. Chem. B.* **2007**, *111*, 8305.
- (8) Cornell, D. G.; Patterson, D. L., *J. Agric. Food. Chem.* **1989**, *37*,1455.
- (9) Bos, M.; Nylander, T., *Langmuir* **1996**, *12*, 2971.
- (10) Sánchez-González, S.; Ruiz-García, J.; Gálvez-Ruiz, M. J. *J. Colloid Interface Sci.* **2003**, *267*, 286.
- (11) Quinn, P. J.; Dawson R. M. C. *Biochem. J.* **1969**, *113*, 791.
- (12) Xicotencatl-Cortes, J.; Mas-Oliva, J.; Castillo, R. *J. Phys. Chem. B* **2004**, *108*, 7307.

- 1  
2  
3 (13) Möbius, D.; Miller, R.; Nylander, T. Protein at Liquid interfaces; Elsevier: Netherlands,  
4  
5 1998.  
6  
7 (14) Damodaran, S. *Food proteins: an overview*. In *Food Proteins and their Applications*,  
8  
9 Damodaran, S., Paraf, A. Eds.; Marcel Dekker Inc.: New York, 1997; pp1-24.  
10  
11 (15) Segura-Nieto, M; Barba de la Rosa, A. P.; Paredes-López, O. *Biochemistry of Amaranth*  
12  
13 *Proteins*, pp 75-106, in *AMARANT Biology, Chemistry and Technology*, ed. Octavio Paredes-  
14  
15 López, CRC Press, USA.  
16  
17 (16) Barba de la Rosa, A. P.; Gueguen, J.; Paredes-López, O.; Viroben, G. *J. Agric. Food Chem.*  
18  
19 1994, 40, 931.  
20  
21 (17) Lösche, M.; Sackmann, E.; Möhwald, H. *J. Phys. Chem.* **1983**, 87, 848.  
22  
23 (18) R.M. Weis and H.M. McConnell, *Nature (London)* **310**, 47 (1984).  
24  
25 (19) Henón, S.; Meunier, J. *Rev. Sci. Instrum.* **1991**, 62, 36.  
26  
27 (20) Qiu, X. ; Ruiz-Garcia, J. ; Stine, K. J. ; Knobler, C. M. ; Selinger, J. V. *Phys. Rev. Lett.*  
28  
29 **1991**, 67, 703.  
30  
31 (21) Ruiz-Garcia, J.; Qiu, X.; Tsao, M. W.; Marshall, G.; Knobler, C. M.; Overbeck, G. A.;  
32  
33 Möbius, D. *J. Phys. Chem.* **1993**, 97, 6955.  
34  
35 (22) Rodríguez-Patino, J. M.; Carrera Sánchez, C.; Molina Ortiz, S. E.; Rodríguez Niño, M. R.;  
36  
37 Añón, M. C. *Ind. Eng. Chem. Res.* **2004**, 43, 1681.  
38  
39 (23) Cejudo Fernández, M.; Carrera Sánchez, C.; Rodríguez Niño, M. R.; Rodríguez Patino, J.  
40  
41 *M. Biomacromolecules.* **2006**, 7, 507.  
42  
43 (24) Knoll, M.; Ruska, E. *Z. Phys.*, **1932**, 78, 318.  
44  
45 (25) Ruska, E. *Rev. Mod. Phys.* **1987**, 59, 627.  
46  
47 (26) Binning, G.; Quate, C. F.; Gerber, Ch. *Phys. Rev. Lett.* **1986**, 56, 930.  
48  
49 (27) Cornell, D. G.; Carrol R. J. *J. Colloid and Interface Sci.* **1985**, 108, 226.  
50  
51 (28) Nakamura, S.; Ankara, H.; Krafft, M. P.; Shibata, O. *Langmuir* **2007**, 23, 12634.  
52  
53  
54  
55  
56  
57  
58  
59  
60

- 1  
2  
3 (29) Ruíz-García, J.; Moreno, A.; Brezesinski, G.; Möhwald, H.; Mas-Oliva, J.; Castillo, R. *J.*  
4  
5 *Phys. Chem. B* **2003**, *107*, 11117.  
6  
7 (30) Valencia-Rivera, D. E.; Basaca-Loya, A.; Burgoa, M. G.; Gutierrez-Millan L.E.; Cadena-  
8  
9 Nava, R. D.; Ruiz-García, J. ; Valdez, M. A. *J. Colloid Interface Sci.* **2007**, *316*, 238.  
10  
11 (31) Barba, A. P.; Gueguen, J.; Paredes-López, O.; Viroben, G.; *J. Agric. Food Chem.* **1992**, *40*,  
12  
13 931.  
14  
15 (32) Krüger, P.; Lösche, M. *Phys. Rev. E.* **2000**, *62*, 7031.  
16  
17 (33) Weiss, R.M.; McConnell, H. M. *J. Phys. Chem.* **1985**, *89*, 4453.  
18  
19 (34) Aroti, A.; Leontidis, E.; Matselva, E.; Brezesinski, G. *J. Phys. Chem. B* **2004**, *108*, 15238.  
20  
21 (35) Carrera, C.; Molina, S. E.; Rodríguez, M. R.; Añon, M. C.; Rodríguez, J. M. *Langmuir*  
22  
23 **2003**, *19*, 7478.  
24  
25 (36) Ruiz-Garcia, J.; Gamez-Corrales, R.; Ivlev, B. I. *Physica A* **1997**, *236*, 97; *Phys. Rev. E*,  
26  
27 **1998**, *660*, 58.  
28  
29 (37) Heat, J. R.; Knobler, C. M.; and Leff, D.V., *J. Phys. Chem. B* **1997**, *101*, 189.  
30  
31 (38) Ning L; and Villota, R., *J. Food Proc. Preserv.* **2007**, *18*, 421.  
32  
33  
34  
35  
36  
37  
38  
39  
40  
41  
42  
43  
44  
45  
46  
47  
48  
49  
50  
51  
52  
53  
54  
55  
56  
57  
58  
59  
60

## FIGURE CAPTIONS

Fig. 1. (Left panel)  $\Pi$  vs  $A$  isotherms of L-DPPC monolayers spread on a phosphate buffered water subphase (pH 8.0 and 25°C, solid symbols) and on a deionized water subphase (pH~5.5 and 25°C, open symbols). (Right panel) BAM images corresponding to the arrow positions in the left panel. a) Chiral LC domains on a continuous LE phase on a water subphase; b) The number and size of the three armed chiral domains of the LC phase increase. c) Pure LC phase. d) LC domains on a continuous LE phase observed on a phosphate buffered water subphase. Note that the LC domains do not longer have the chiral shape but they have sharp edges, which are more noticeable in e). f) The LC domains are coalescing to form a continuous LC single phase. Each image size is 462  $\mu\text{m}$  x 564  $\mu\text{m}$ .

Fig. 2. (Left panel)  $\Pi$  vs  $A$  isotherms of globulin 11S film spread onto a deionized water subphase at  $T=25^\circ\text{C}$  (solid symbols). Globulin 11S spread onto a phosphate buffered water subphase at  $T=25^\circ\text{C}$  (open symbols). (Right panel) BAM images a) y b) Globulin 11S spread on deionized water subphase showing a homogeneous phase with small three-dimensional aggregates; c) Collapse of the globulin 11S monolayer on water subphase. d), e) and f) Globulin 11S monolayer deposited on a phosphate buffered water subphase, bright points and foam-like structure must correspond to three dimensional protein structures. Each image size is 462  $\mu\text{m}$  x 564  $\mu\text{m}$ .

Fig. 3. (Left panel)  $\Pi$  vs  $A$  isotherms of globulin 11S monolayers obtained 6 hrs after protein injection below the air/buffer (pH 8.0 and 25°C, solid symbols) and the air/water (pH ~ 5.5 and 25°C, open symbols) interfaces. (Right panel) BAM images corresponding to the arrow positions in the left panel. a)-b) Coexistence between the LE-G phases on the water subphase; the small circular domains correspond to the LE phase and the dark, continuous area is the G phase. c) Continuous LE phase with small three-dimensional aggregates. d)-f) An almost homogeneous and continuous protein film is formed at all surface pressures, when the protein is injected below the air/buffer interface and allow to diffuse towards it. Each image size is 462  $\mu\text{m}$  x 564  $\mu\text{m}$ .

Fig. 4.- (Left panel)  $\Pi$  vs  $A$  isotherms of L-DPPC monolayer spread on a globulin film at the air/water interface ( $T=25^\circ\text{C}$ , open symbols) and on a globulin film at the air/buffer interface ( $T=25^\circ\text{C}$ , solid symbols). (Right panel) BAM images corresponding to the arrow positions in the left panel. a) Coexistence between a L-DPPC-rich region and mixture region. L-DPPC domains do not show chiral features due to protein presence. Note that the domain on the top left corner present a fingering instability; b) coalescence of L-DPPC domains, the continuum formed by these domains present internal anisotropic structure due to molecular tilt of the L-DPPC molecules; c) Clear separation into a protein-rich (white) region showing fingering and L-DPPC-rich (dark) region. d) At low surface pressures L-DPPC and Globulin mix well; e) Coexistence between a protein rich-domain, brighter top domain, and a L-DPPC-rich phase, bottom dark region; f) image clearly showing a protein-rich domain (white), a L-DPPC-rich region (dark) and a mix domain of both protein and L-DPPC (gray domain). Each image size is 462  $\mu\text{m}$  x 564  $\mu\text{m}$ .

Fig. 5. (Left panel)  $\Pi$  vs  $A$  isotherms of a Langmuir monolayer of L-DPPC when globulin11S was injected below it. L-DPPC was spread on the water subphase ( $T=25^\circ\text{C}$ , open symbols) and on the buffer subphase ( $T=25^\circ\text{C}$ , solid symbols). (Right panel) BAM images corresponding to the arrow positions in the left panel. a)-c) LC domains of L-DPPC monolayer spread on water; the domains show fingering instabilities. In

1  
2  
3 addition, one can observe small white dots corresponding to protein aggregates; in c), the protein concentrates  
4 mainly in the LE-LC interface of the L-DPPC monolayer. d)-f) L-DPPC domains on buffer subphase; the LC  
5 and LE phases of L-DPPC show small white dots imbedded corresponding to the protein; in f), the protein  
6 aggregates at the LE-LC interface, but the protein aggregates are smaller than in experiments done on water  
7 subphase. Each image size is 462  $\mu\text{m}$  x 564  $\mu\text{m}$ .  
8  
9

10 Fig. 6. AFM images of L-DPPC transferred onto mica at  $\Pi = 14$  mN/m. a) transferred from a deionized water  
11 subphase. The continuous phase corresponds to the LC phase while the phase made of small, darker circles  
12 and lines corresponds to a metastable LE phase. The height of each phase with respect to the mica is  $\sim 2.8$  nm  
13 and  $\sim 2.3$  nm for the LC and LE phases, respectively. Note that the curved lines come from the healing  
14 process among the chiral LC domains. b). transferred monolayer from the buffer subphase. In this case the  
15 healing defect lines are not so curved as in a). Moreover, the height difference between the phases is bigger;  
16 the height of the LC, continuous phase, is  $\sim 2.6$  nm, while the darker, metastable LE phase, is  $\sim 1.6$  nm.  
17  
18

19 Fig. 7. AFM images of globulin 11S transferred onto mica when the protein was spread on deionized water  
20 (a-b) and buffer subphases (c-d). The transfer pressure was  $\Pi = 18$  mN/m. a) Figure shows bright dots that  
21 correspond to globular structures of different sizes; b) is a zoom where one can clearly observe these globular  
22 structures forming a multilayer. c) Transferred film from a buffered water subphase. In this case, it was  
23 observed similar structures than those observed on water subphase, but the globular structures have smaller  
24 dimensions; d) Globular structures mostly formed by individual proteins.  
25  
26

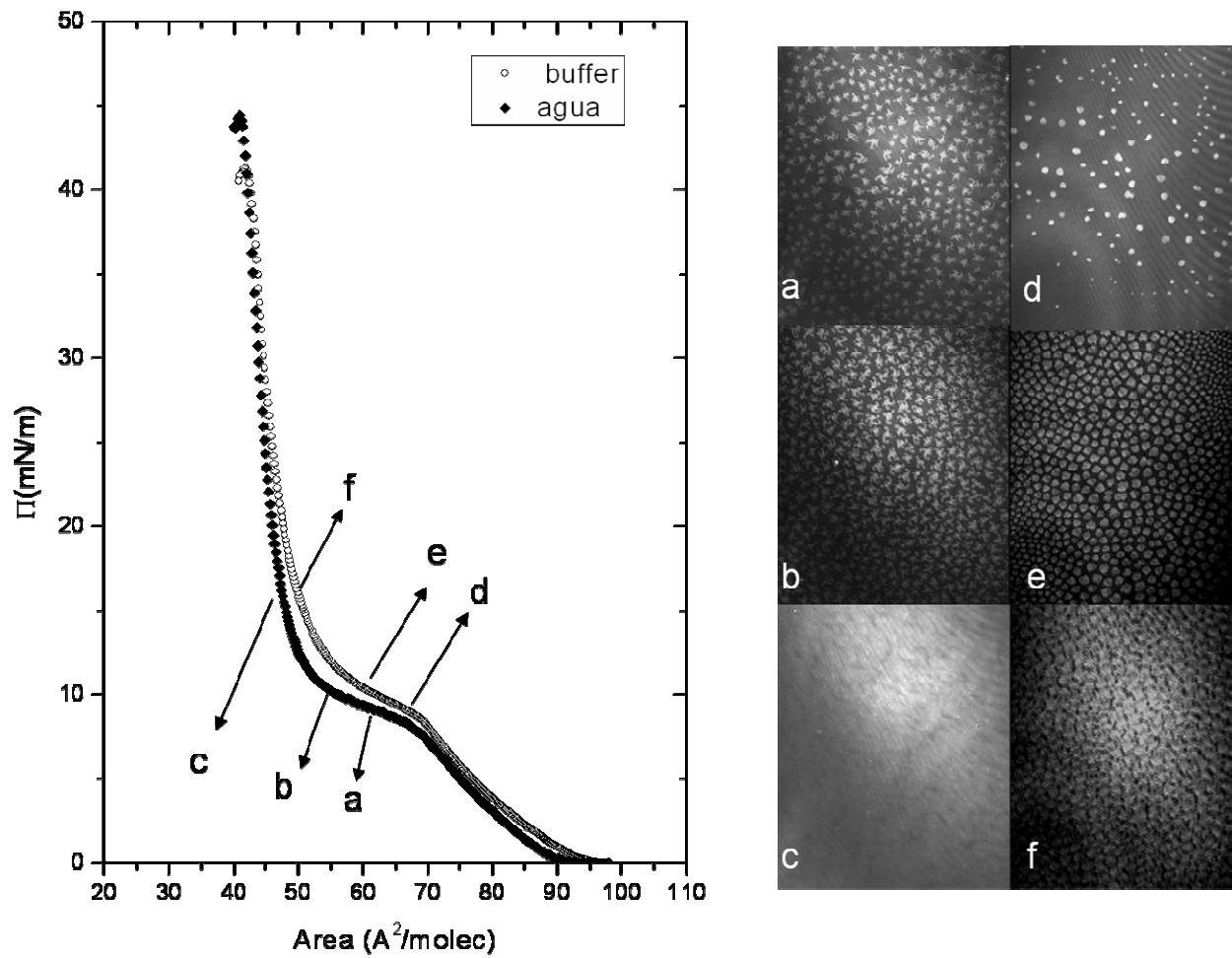
27 Fig. 8. AFM images of globulin 11S transferred onto mica when the protein was injected below the interface  
28 and allowed to diffuse for six-hours towards the interface. The transfer was done at  $\Pi = 8$  mN/m a) and b)  
29 air/water interface; c) and d) air/buffer interface. On both subphases a homogeneous film is formed; on buffer  
30 the film shows a remarkable crystalline-like order. The inset in d) is the Fourier transform of the figure.  
31  
32

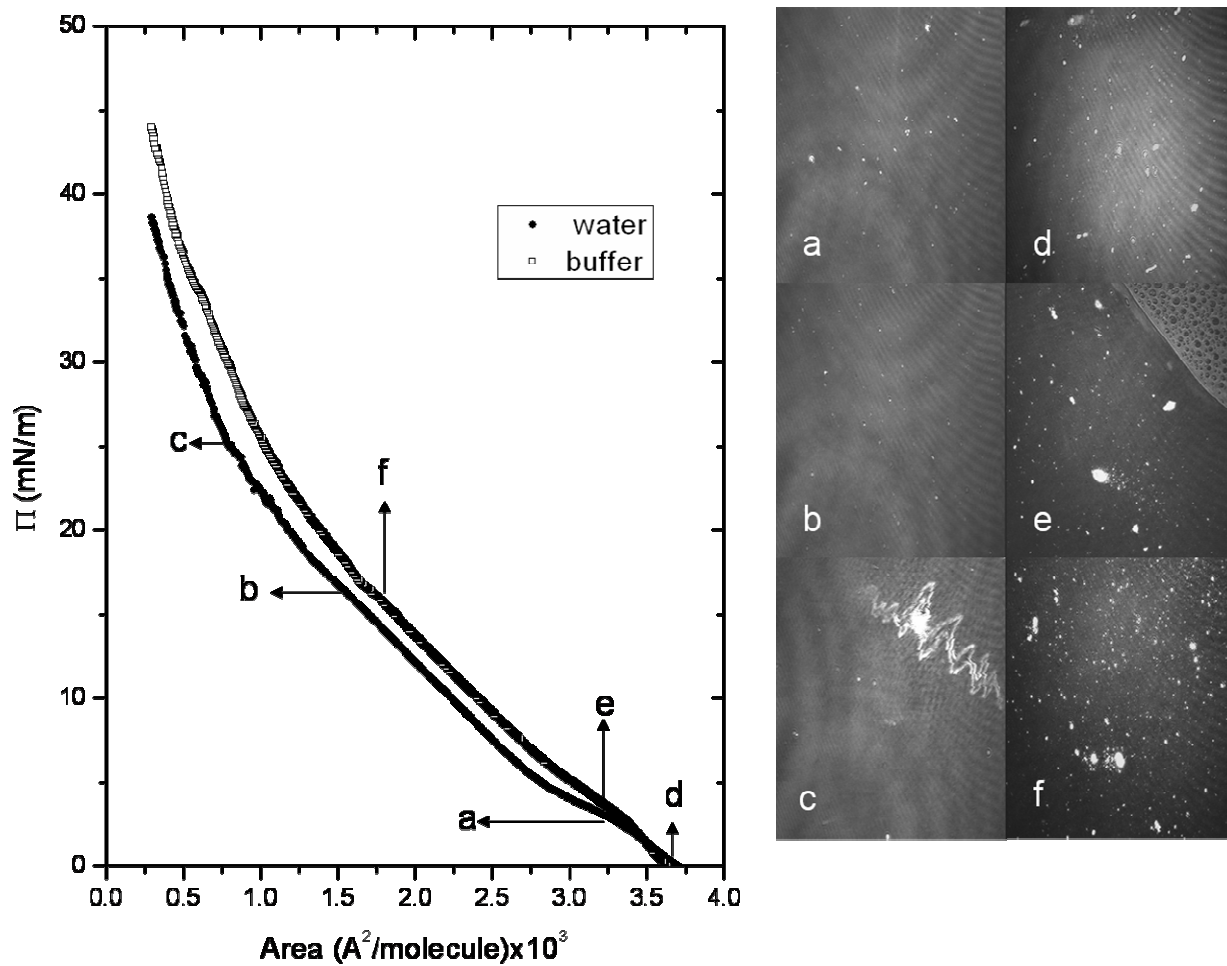
33 Fig. 9. AFM images of a mixture of globulin 11S and L-DPPC transferred onto mica when: a)-c) globulin was  
34 deposited on deionized water subphase and d)-f) globulin was deposited on a buffer subphase; L-DPPC was  
35 immediately deposited in both cases. The transference pressure was  $\Pi = 18$  mN/m. a) Coexistence between  
36 protein-rich domains and L-DPPC-rich region; b) Close-up of image a) where one can see that the large  
37 domain at the bottom presents internal structure, i. e. holes (see also Fig. 10); c) Protein rich domains show  
38 globular internal structure; d)-f) the mixture shows a fracture film; apparently L-DPPC connects the protein  
39 globules. In addition, three dimensional aggregates are common.  
40  
41

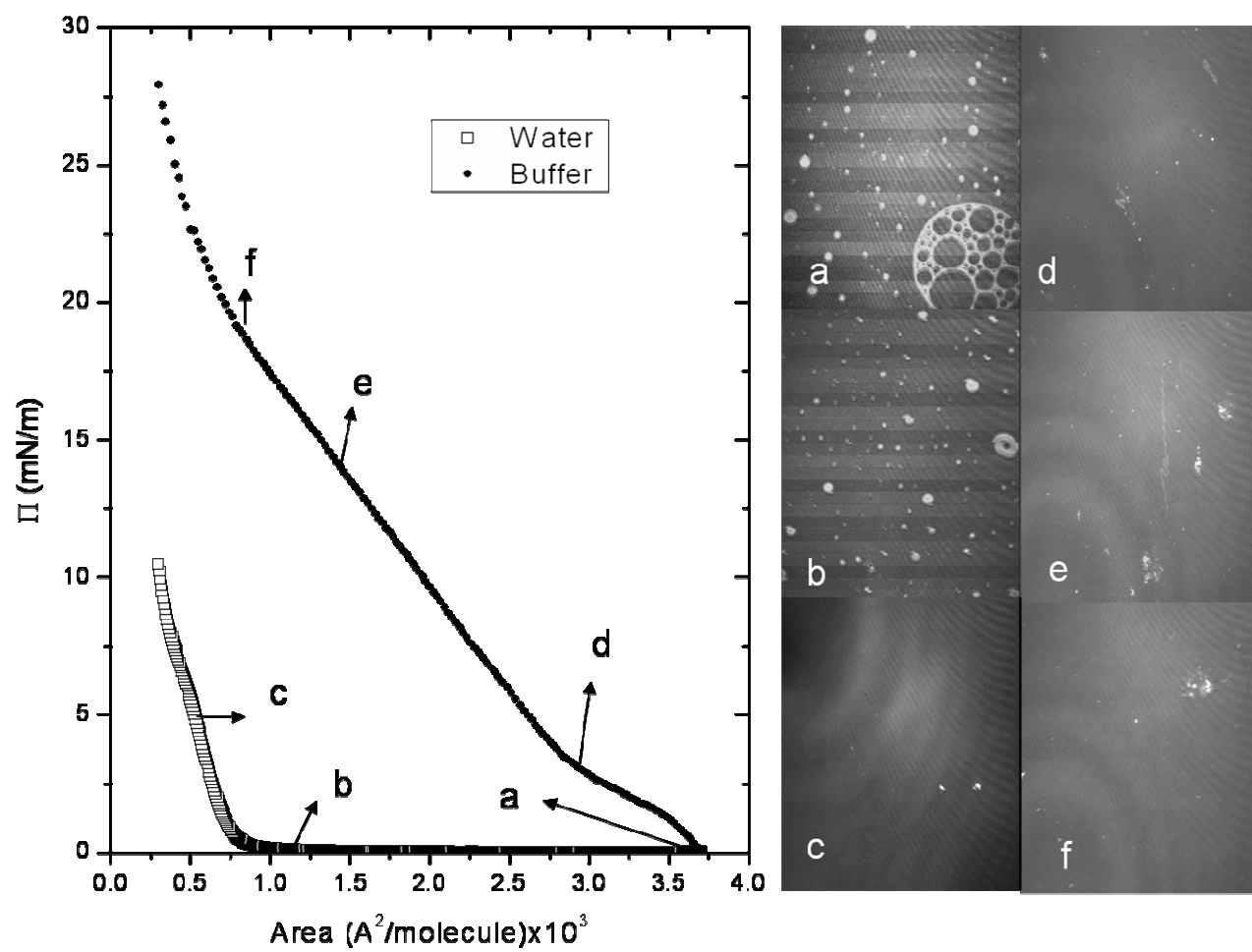
42 Fig. 10. AFM images of a mixture of globulin 11S and L-DPPC transferred on mica. Globulin was deposited  
43 on deionized water subphase and immediately L-DPPC was spread. Transference was done at a pressure  $\Pi =$   
44 18 mN/m. Image shows aggregates with a hole at the center, these aggregates have an average size of  $22.38 \pm$   
45 1.55 nm, and the average size of the holes is  $8.1 \pm 1.19$  nm.  
46  
47

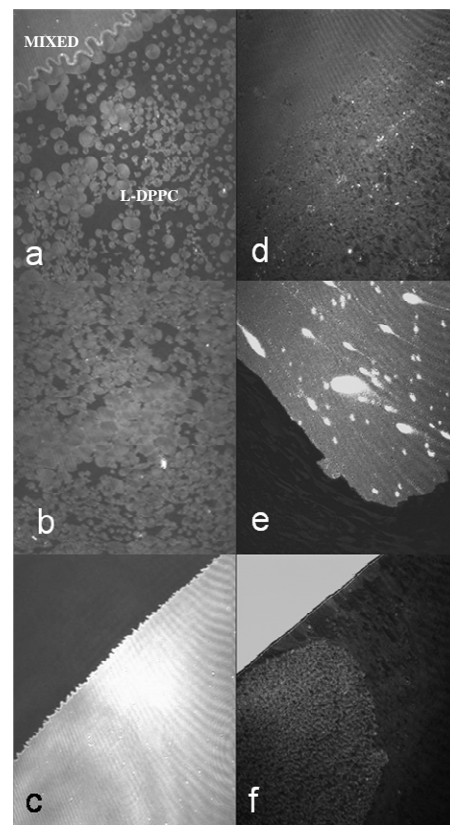
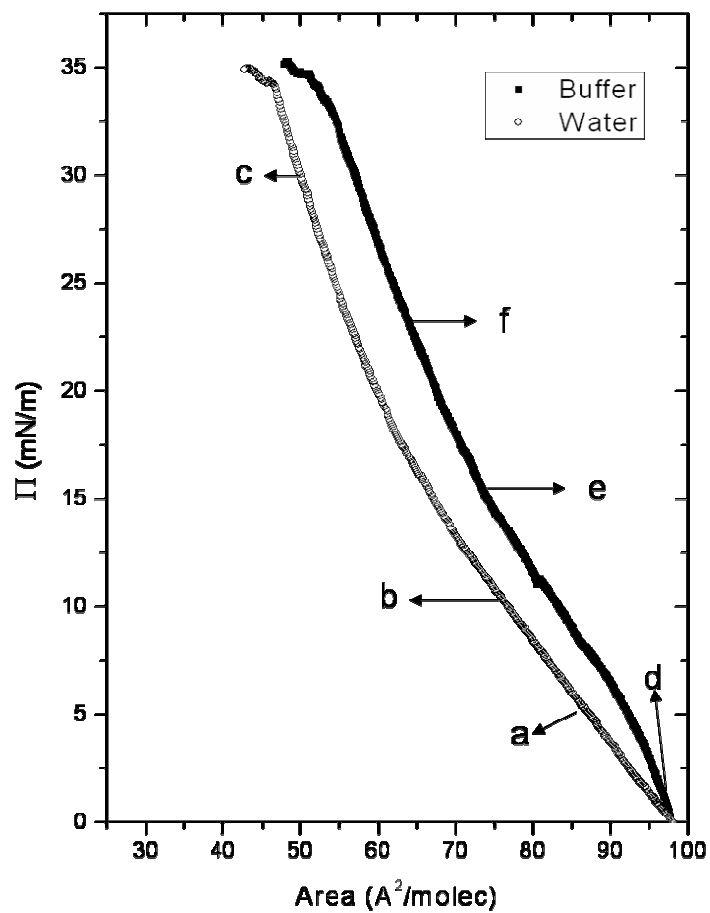
48 Fig. 11. Typical AFM images of a mixture of globulin 11S and L-DPPC transferred onto mica when: a)-c)  
49 globulin was injected below the water subphase and d)-f) globulin was injected below the buffer subphase; L-  
50 DPPC was deposited before injection of the protein in both cases. The transference pressure was  $\Pi = 18$   
51 mN/m. a)-c) a granular mixture is formed: the protein shows a globular structure and penetrates the L-DPPC  
52 monolayer. d)-f) the LC domains of L-DPPC are irregular and much less protein globules are evident.  
53  
54  
55  
56  
57  
58  
59  
60

## FIGURES

Figure 1 Garcia-Gonzalez *et. al.*

Figure 2. Garcia-Gonzalez *et. al.*

Figure 3. Garcia-Gonzalez *et. al.*

Figure 4.- Garcia-Gonzalez *et. al.*

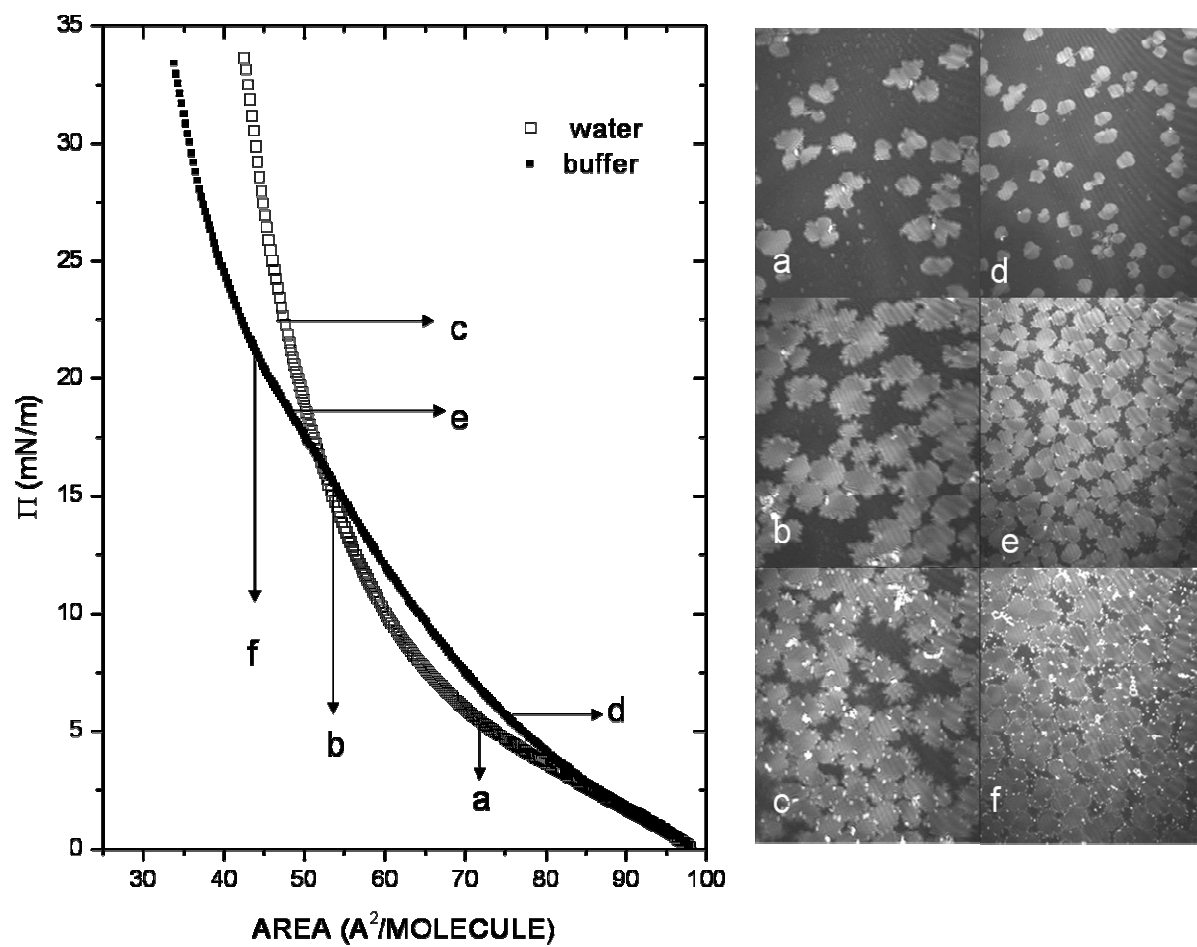


Figure 5. Garcia-Gonzalez *et. al.*

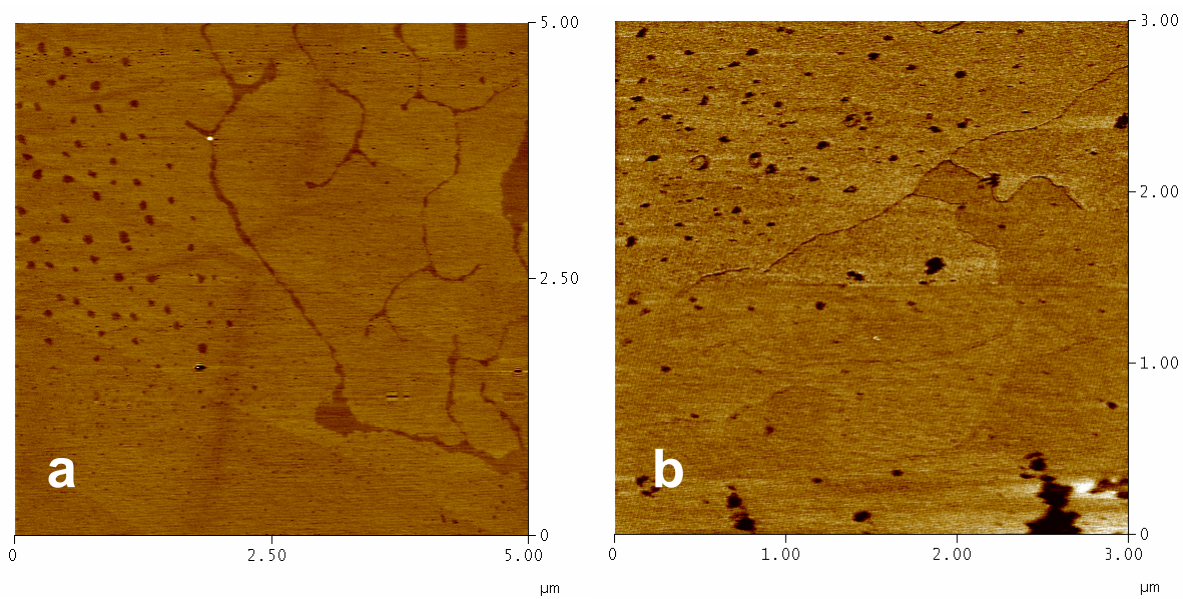


Figure 6. Garcia-Gonzalez *et. al.*

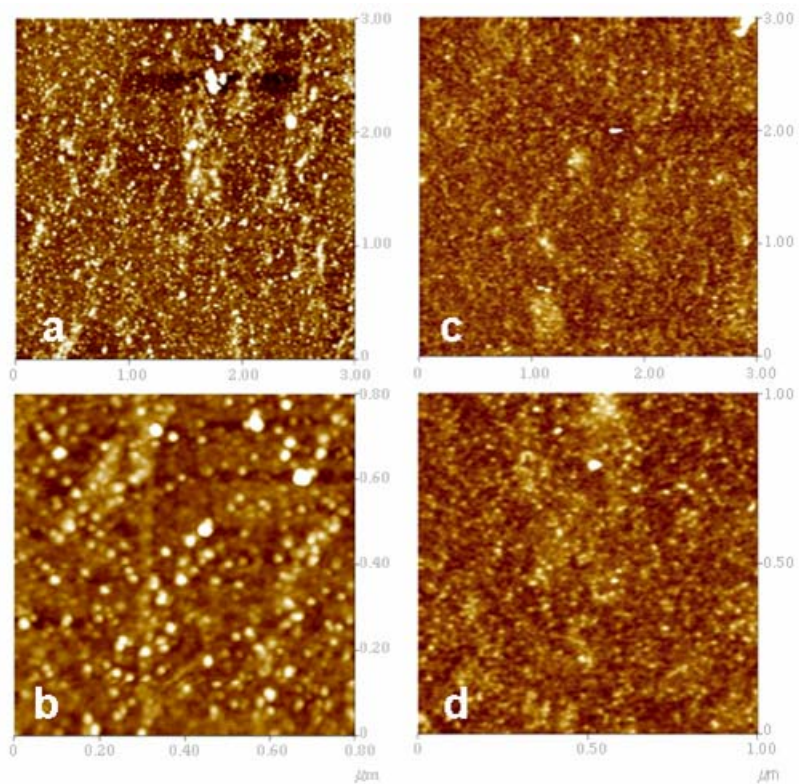


Figure 7. Garcia-Gonzalez *et. al.*

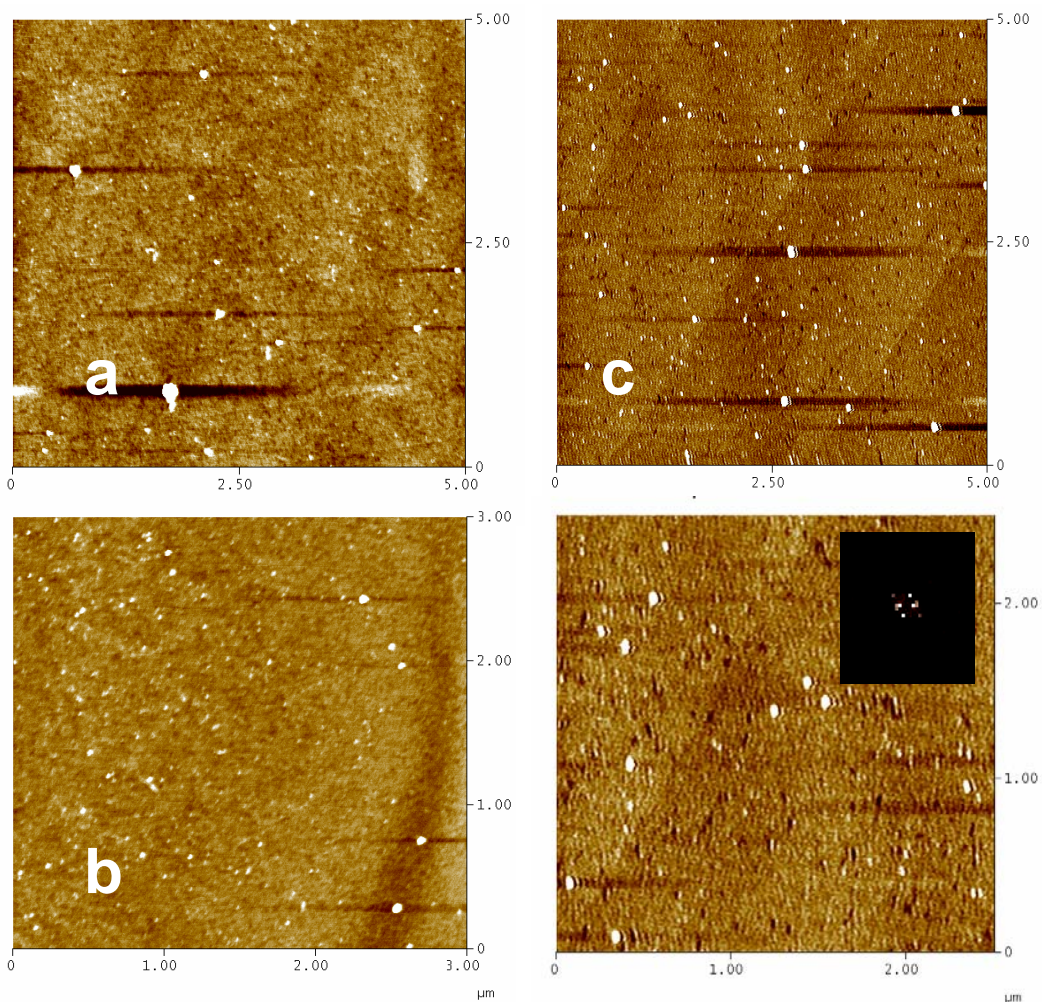


Figure 8. Garcia-Gonzalez *et. al.*

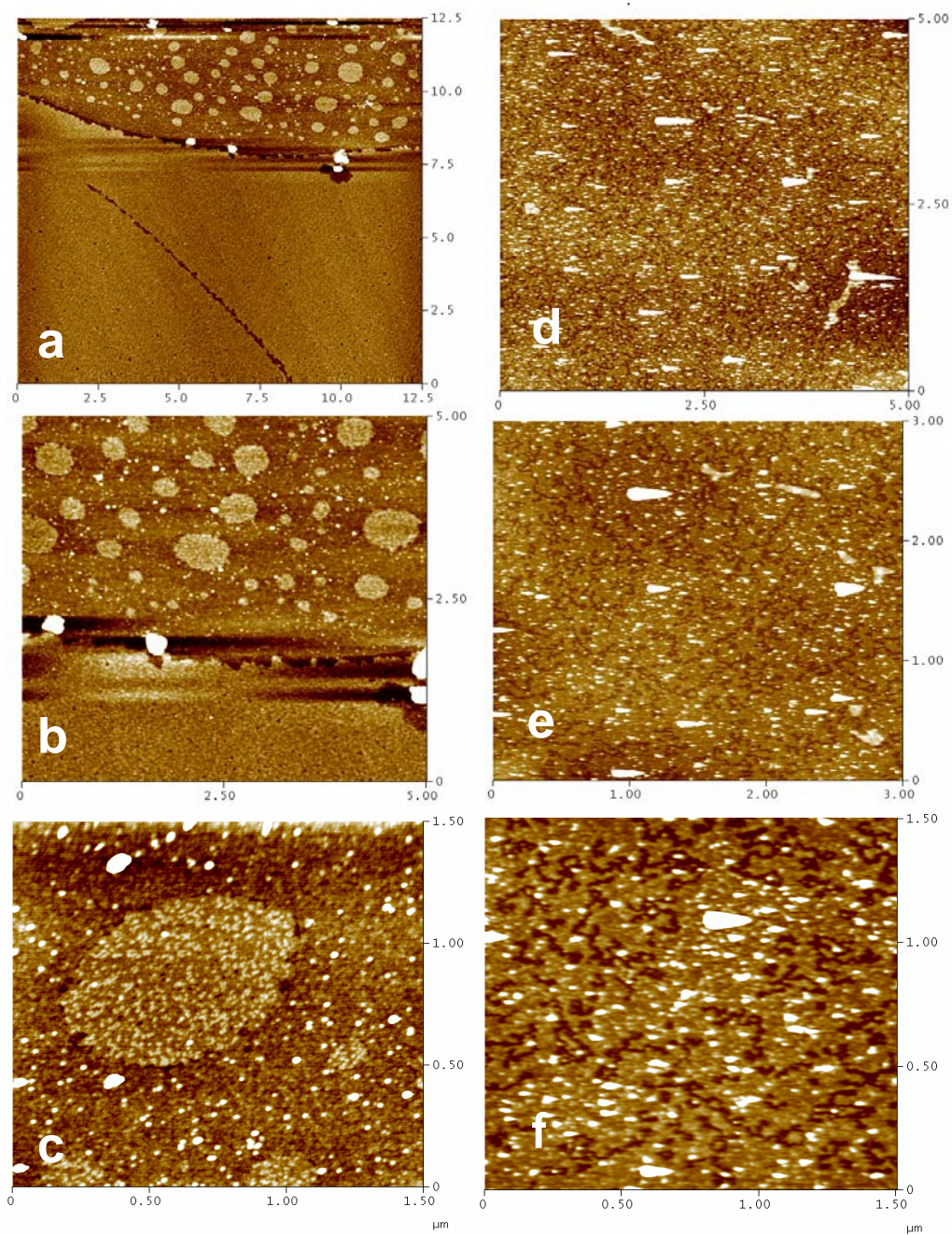


Figure 9. Garcia-Gonzalez *et. al.*

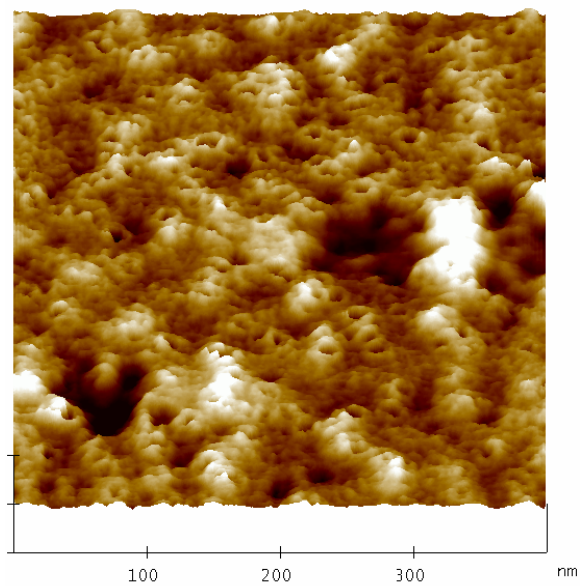


Figure 10. Garcia-Gonzalez *et. al.*

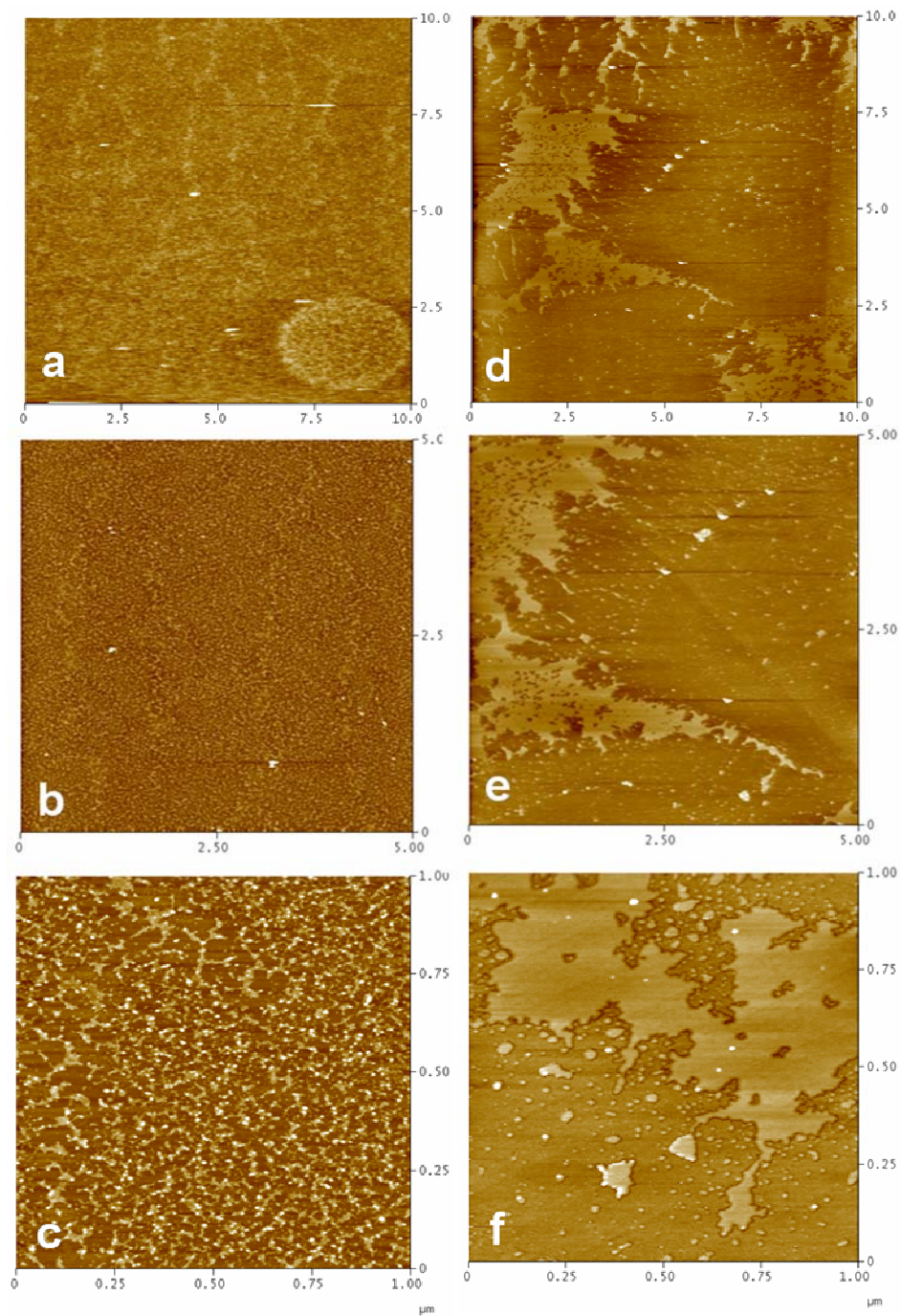


Figure 11. Garcia-Gonzalez *et. al.*